1D-CNN: One Dimensional Convolution Neural Network-based Electroencephalogram (EEG) Signals Classification with Efficient Artifact Removal for Real-Time Medical Applications

Padmini Chattu[1,*], Dr. C.V.P.R. Prasad[2]

[1] Research Scholar, Acharya Nagarjuna University, Nagarjuna Nagar, Guntur, A.P, India

[2] Research Supervisor, Acharya Nagarjuna University, Nagarjuna Nagar, Guntur, A.P, India

Abstract

Mental task detection and classification employing solo/restricted channel(s) electroencephalogram (EEG) signals in actual time perform a significant part in the pattern of mobile brain-computer interface (BCI) and neurofeedback (NFB) schemes. Nevertheless, the actual time registered EEG signals remain frequently adulterated with noises like ocular artifacts (OAs) and muscle artifacts (MAs) that decline the handmade features extracted out of EEG signal leading to insufficient detection and classification of mental tasks. Hence, we analyse the employment of the latest deep learning approaches that in no way need whatsoever physical feature extraction or artifact repression phase. This study proffers a one-dimensional convolutional neural network (1D-CNN) framework for mental job detection and classification. The proffered framework's strength can be analysed employing artifact-free and artifact-adulterated EEG signals obtained out of publicly accessible datasets especially the Emotiv EPOC headset. It is observed that the proffered 1D-CNN attains 0.992 of accuracy, 0.993 of precision, 0.9905 of recall, 0.0065 of FPR, and 0.992 of F-measure. Correlative execution assessment exhibit that the proffered framework surpasses prevailing techniques not merely concerning classification precision yet as well as in strength opposing artifacts.

Keywords - Pre-processing, artifacts, EEG, CNN, feature extraction, classification, brain, electrodes.

1. Introduction

EEG uses electrodes, which are usually placed on the scalp, to record the electrical activity of the cerebral cortex. This method is extensively used to diagnose sleep problems and epilepsy in medical settings [1]. In the real-time BCI applications, medical practitioners and EEG gains attracting performance for analysis [2]. In actual circumstances, however,

EEG signal are subjected to different distortion in terms of biological and environmental abnormalities [3]. Unwanted signals [4], which comprises of the non-cerebral EEG electrodes and recorded [5] are referred to as artefacts. Environmental artefacts [6] and biological artefacts [7] are the two types of artefacts. Environmental artefacts are signals that originate from outside the human interference due to movement of electrodes occurs from the external devices such as poer line or electric motors [8], whereas the signal with the biological artifacts arises due to non-cerebral sources in the human body for the ocular and cardiac activity. Consequently, EEG signal with the BCI application degrades the artefacts in terms of biological and environmental factors [9].

Machine learning and pattern identification techniques applied in the EEG data. In neural classification, classical supervised learning methods such as linear discriminant analysis (LDA) [10], decision tree and Support vector machine (SVM) which uses the canonical correlation analysis (CCA) for the elimination of artifacts. The feature dimensionality is minimized with the ICA, LFDA and PCA.

In neural classification applications, neural networks were not as popular as they are now because of practical difficulties such as excessive computation times and issues with vanishing/exploding gradients [11]. Researchers studying neural networks may now examine deep learning designs (neural network topologies with at least two hidden layers) because of recent advances in graphics processing units (GPUs), which are both affordable and powerful [12]. Because of these developments, deep learning has been more popular and useful over the last decade[13]. A range of previously challenging domains, including photographs, videos, audio, and text were improved as a result of this technology. As a result, neural networks are assumed to need less prior knowledge of the dataset in order to function well [14-15].

Medical imaging, which often comprises of the larger dataset for examination and analysis for the effective performance analysis. Deep learning model utilized in the EEG signal for the utilized decoding and classification, those are associated with the low signal to noise ratios (SNRs) and higher data dimensionality for the increased availability with the massive EEG datasets [16]. Complex architecture and input signals such as time-frequency components in 2D or 3D form in the single or multi-channel EEG with the CNN-based workload classification model [17-18]. A 1D-CNN architecture is presented in this research to detect and categorise mental processes from single EEG channels. The contribution of this wok are as follows,

- To remove the noise and artifacts using Morelette wavelet based pre-processing method and extract the relevant feature in the EEG signal in raw format using CNN model.

- To design low complex subject-independent architecture based on 1D-CNN and compare it with the traditional method by using Emotiv EPOC headset dataset.

The rest of this chapter is ordered as follows - Section 2 mentions a few existing research works, Section 3 shows the proposed approach and methodologies, Section 4 exhibits the experimental outcomes and discussion, and, finally, Section 5 ends up with conclusion and future work.

2.Literature works

In [19] developed a model to evaluate the physical or signal interference in the EEG artifacts. The developed model integrates the decomposition model with the Regenerative Multi-Dimensional Singular Value Decomposition (RMD-SVD). The proposed model uses the multivariate data Independent Component Analysis (ICA) data from the acquired signal. With the application of the regenerative reference input signal is constructed and evaluated with singular value decomposition. The performance analysis expressed that the proposed model exhibits improved performance in terms of SNR, PSNR, MSE, and so on. Additionally, the proposed model exhibits higher elimination efficiency with consideration of the different filters. In [20] presented a model to evaluate the EEG epoch probability based on consideration of the statistical features such as entropy, kurtosis, skewness, and index of a periodic waveform. The developed model to computes the features of the EEG artifacts based on the computation of the threshold values. The proposed model exhibits efficient performance in the removal of artifacts through automated methods. The developed model is efficient and suitable for real-time applications.

In [21] constructed a supervised artifact elimination method in EEG based on consideration of chunks with the utilization of the independent component analysis. To eliminate the ocular artifacts discrete wavelet transform is applied for the 29 subjects based on the consideration of gestures such as walking and facial expression in the video. The EEG features are extracted based on the consideration of the 13 morphological features for the classification of the eye chunks' movements. The movements of the eye in the EEG signal are processed with the elimination of the morphological distortion in the signals. The developed method exhibits significant performance in terms of mutual information, kurtosis, correlation, phase difference, and computational time. The developed model exhibits

improved sensitivity and specificity for robustness. In [22] proposed an intelligent hybrid model for the removal of artifacts in the EEG signal. The proposed model uses the training and testing evaluation with the One-Dimensional Convolutional Neural Network (1D-CNN) integrated with the Spider monkey-based Electric Fish Optimization model (SM-EFO). The proposed SM-EFO uses the 1D-CNN for parameter tuning. The experimental analysis is performed with the conventional benchmark datasets to improve the performance. The proposed SM-EFO model exhibits improved performance than the conventional techniques. In [23] presented an efficient modular generative adversarial network (GAN) to improve network performance with an appropriate training strategy for the EEG artifacts removal. The proposed model exhibits the representation ability in the model with a reliable BCG generator for artifact removal. The proposed GAN model eliminates the requirement of hardware and additional reference signal requirement. The comparative analysis stated that the proposed GAN model significantly eliminates the BCG artifacts to retain EEG information. In [24] developed a computational intelligence model for identification and differentiation artifacts in the EEG signal. The proposed computational intelligence model uses the Residual Deep Neural Network model in EEG signals with data collected from 79 infants. With prediction and statistical analysis of the validated features, the dataset is processed with the average probability with the temporal window features. The developed residual deep neural network exhibits the accuracy of 95% with computation of the median accuracy. The validation and misclassification accuracy is estimated between the range 1% - 11% with the validation set of 87%.

In [25] developed a model for EEG artifacts integrated with canonical correlation analysis (OCA) integrated with noise adjusted principal component transform (NAPCT) for the elimination of the artifacts observed through eye blinks. The estimated features provide the average signal-to-noise ratio of 3.616 with the root means square error value of 42.456 for the EEG artifacts data. The estimated correlation coefficient is computed as 0.8839 with the mutual information value of 1.1546. The proposed approach effectively exhibits the EEG artifacts for the manual intervention for elimination of the EEG artifacts. In [26] presented a one-dimensional residual convolutional neural network (1D – ResCNN) for denoising EEG signals. The developed 1D – ResCNN model is involved in the estimation of the noisy and clean EEG signal. The developed 1D – ResCNN with the elimination of the automated noise removal in the contaminated EEG signal. The evaluation of the EEG model is based on the consideration of the CHB – MIT database. The results expressed that the proposed 1D –

ResCNN model exhibits improved performance for the RMSE and SNR values. In [27] constructed a signal decomposition model for the EEG artifacts. The developed model exhibits the estimation of the variational model decomposition (mVMD) model with the limited intrinsic model function in the estimation of the EEG signal. The EEG signal is involved in exploitation of the EEG artifacts for the identification of the components with estimated QRS reference estimation in the signal. The developed mVMD model exhibits an average correlation value of 97%.

Conventional machine learning and subject-dependent handmade features are the most common methods for identifying and classifying mental tasks. Due to considerable structural and functional variability across participants and EEG non-stationarity, these approaches may not be generalizable across persons and datasets. A strategy that uses deep learning to learn features from raw data during training may be able to solve this problem. In table 1 presented the summary of the literature in EEG artifacts.

Table 1: Summary of Literature

Reference	Aim	Outcome	Limitation
[19]	developed model to evaluate the physical or signal interference in the EEG	Increased SNR, PSNR, MSE	Classification is not performed
[20]	Estimates the EEG artifacts through probability threshold	The proposed model exhibits superior performance for real-time applications	Complexity is higher
[21]	Developed a supervised artifact removal	Improved sensitivity and specificity	Accuracy is not adequate
[22]	Proposed a SM-EFO model	Increases the overall performance	Suitable for benchmark dataset alone
[23]	Developed a GAN model	Eliminates the hardware requirement	Classification is not adequate
[24]	Constructed computation intelligence residual neural network	Accuracy is estimated as 95%	The estimated error is minimal
[25]	Presented a canonical	provides an average signal	Classification

	correlation analysis (CCA) and noise adjusted principal component transform (NAPCT)	to noise ratio and root mean square error values of 3.616 & 42.456	value is not defined
[26]	Constructed a 1D – ResCNN model	Improved SNR and RMSE value	Classification is not performed

3.Methodology

The below figure 1 exhibits the proffered EEG signal classification scheme's overall methodology flow with efficient pre-processing and feature extraction method.
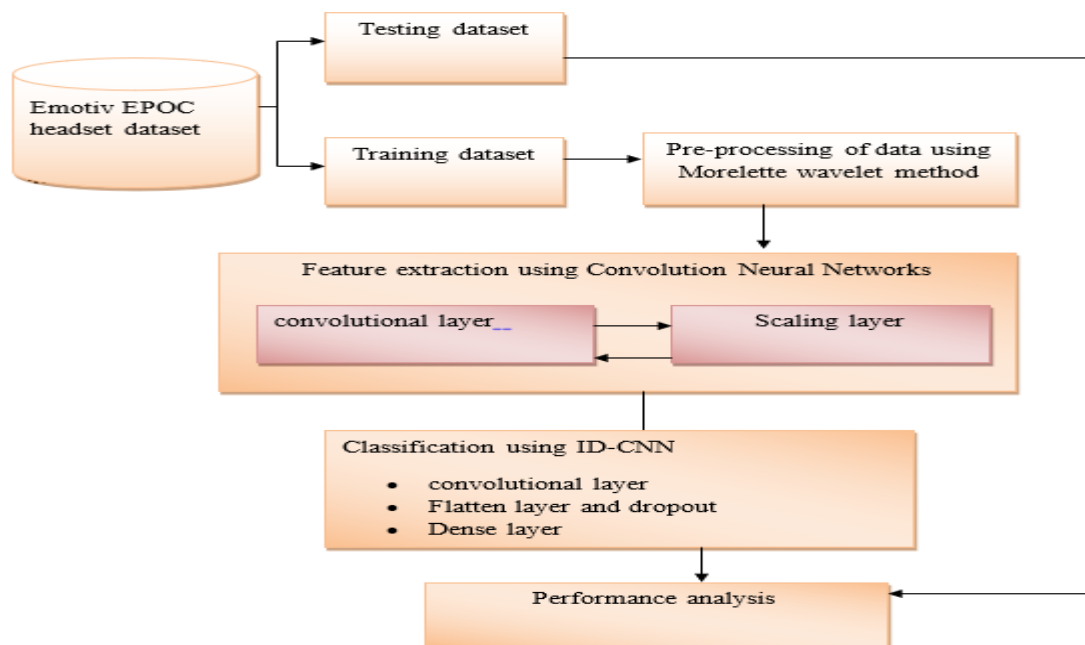

Figure 1. System model for EEG signal classification

Initially, the input database is trained, and during this procedure, the signals are pre-processed employing Morelette wavelet methodology. During pre-processing, the signal is rebuilt, and the noise is eliminated at first; next, the signal is cleared. Such noise elimination signal is provided to feature extraction unit by building CNN framework while convolution layer and scaling layer are present. Then, we train the 1D-CNN framework employing the training database of the classification plan. Subsequent to every epoch, the training precision and deprivation are noticed in the proffered scheme. The execution is evaluated with a few evaluation metrics like accuracy, precision, recall, FR, and F1-score of the proffered scheme.

3.1 Dataset description

The database employed for the experiential assessment is excerpted out of the University of California-Irvine (UCI), a machine-learning repository. The database comprises 15,181 examples of fifteen features. The positioning of the electrode chiefly comprises 5 regions like central (C), frontal (F), occipital (O), parietal (P), and temporal (T). The entire cranium is partitioned as 2 areas – left and right. The former portion comprises the O1, P7, T7, FC5, F3, F7, and AF3 electrodes. Simultaneously, the latter portion comprises O2, P8, T8, F8, FC6, F4, and AF4 electrodes. The vision of fourteen channels (that is, AF3, F7, F3, FC5, T7, P7, O1, O2, P8, T8, FC6, F4, F8, and AF4) and class-based (that is, open and close) EEG signal data for eye situation is performed.

3.2 Pre-processing employing Morelette wavelet methodology

The effectual artifacts elimination out of the EEG signal is needed to be applied by excerpting the majority of the important non-linear attributes despite the intricate and duration-variable signals. Hence, such difficulties should be resolved by embracing a novel EEG artifacts elimination methodology by Morelette wavelet methodology. The Time-frequency domain is portrayed as a wavelet transform. A signal's Morelette Wavelet Transformation is provided by,

$$CWT(a,b) = \frac{1}{\sqrt{|a|}} \int_{-\infty}^{+\infty} X(t)\psi^* \left(\frac{t-b}{a}\right) dt \qquad (1)$$

As per Parseval's theorem, signals remain split up in different levels. This is given by,

$$CD_i = \sum_{j=1}^{N} |Dij|^2, i = 1,\ldots\ldots,1 \qquad (2)$$

$$CA_l = \sum_{j=1}^{N} |Alj|^2 \qquad (3)$$

in which 1 i, ..., 1 remains the wavelet decomposition from level 0 to level 1. N portrays the sum coefficients of each decomposition level. CDi and CA portray the energy of the feature and imprecise at decomposition level i and level 1accordingly. The variance conservation and imprecise decorrelation attributes of the Morelette wavelet transform are employed to build an arithmetical test for variance homogeneity in lengthy memory procedures. This test relies upon the theory that, for a provided duration sequence $x_1, x_2, \ldots x_n$, every series of wavelet

coefficients $w_{j,t}$ for x_t imprecise samples of 0 mean independent Gaussian haphazard variables have variances $\sigma_1^2, \sigma_2^2, \ldots \sigma_n^2$. The null hypothesis for the test remains:

$$H_0: \sigma_1^2 = \sigma_{2,}^2 = \cdots = \sigma_n^2. \qquad (4)$$

and alternative hypotheses remain of the format

$$H_1: \sigma_1^2 = \sigma_c^2 \neq \sigma_{c+1}^2 \ldots = \sigma_n^2 \qquad (5)$$

in which c portrays an unfamiliar variance change point. The test stat is centered upon the employment of the normalized cumulative total of squares μ_c.

$\mu_c = subj$ which w_j portraysDWT scale j DWT coefficients. μ_c calculates variance accumulation in a duration sequence as a time function. A rotated cumulative variance plot, hence, gives an average of learning the time dependence of the variance of a sequence – when the variance remains static through the time, that is, the null hypothesis is approved, μ_c must raise linearly alongside c at about 45 degrees having every haphazard variable provide a similar variance quantity; contrastingly, when H_0 remains denied, substantial divergence out of 45-degree line would happen.

3.3 Feature extraction by Convolutional Neural Networks

A Scaling Layer (SL) is initially provided that remains a construction block employed for adaptatively excerpting efficient data-driven spectrogram resembling features out of unprocessed EEG signals. Next, a completely CNN-based on the SL is presented.

We contemplate a multiple kernel convolutional layer, which obtains a unidimensional signal having shape sampling points, one remains as input and evolves as output a bidimensional spectrogram resembling feature map having shape sampling points, and scaling levels through the ensuing layer-wise propagation rule.

$$\boldsymbol{H^{output}(l) = \delta(bias\ (l) + downsample(weignt, l) \times H^{input})} \qquad (6)$$

in which $\boldsymbol{H^{input}}$ portrays the input vector having shape duration phases – 1, that is, the unidimensional signal, $\boldsymbol{H^{output}}$ portrays the activations matrix having shape duration phases – scaling levels, that is, the data-driven spectrogram resembling feature map, bias portrays the biases for the multiple kernel produced by scaling a fundamental kernel, $\boldsymbol{\delta(.)}$ portrays an activation function, weight portrays the fundamental kernel out of what the rest of the kernels

will be scaled, and l portrays a hyper-criterion, which regulates the scaling level. Down Sample remains a pooling agent, which downsamples the weight by a mean filter having a dimension two window, performing it one time. It scales the data-driven design weight towards a particular duration for capturing particular frequency-like portrayals out of H^{input}.

Presume that we desire to excerpt features for signal H^{input} in the lth scaling level. At first, the lth scaling level kernel is produced that is scaled out of $weight$ by down sample $weight$. Next, the scaled kernel's cross-correlation agent and H^{input} are executed. Later, the former outcome and the $bias\ (l)$, are added and supply the total to the activation function $\delta(.)$. This total scaling level tsl procedure is reiterated having hyper-criterion' disparate formats l upon zero range to maximal scaling level msl in which the msl remains the lth level, which creates the vector length $downSample\ (weight, l)$ equivalent to one, and the $tsl = msl + 1$. Lastly, the entire excerpted feature vectors are stacked into a two-dimensional tensor for acquiring the data-driven spectrogram-like feature map.

3.4 EEG classification employing deep learning

The layers remain built of an array of neurons. Among them, each layer remains linked to entire neurons in the layer. The last completely linked layers are employed for portraying the anticipation and generating the outcome layer. CNNs are organized for mapping an image data into an output variable that demonstrated very efficient for any anticipation issue incorporating features as an input and considered as go-to methodology. The classification of the CNN framework incorporates every neuron's input that is linked to the local receptive field of the former layer and inclines towards the local feature retrieval. The CNN's prime element remains the convolutional layer. The layers' criteria comprise a kernel, which contains the least responsive deflect yet expands via the total deepness of the input content. The extra convolutional layers we give, the finer output we obtain since every layer lessens the input features' quantity to completely linked layers as illustrated in figure 2.
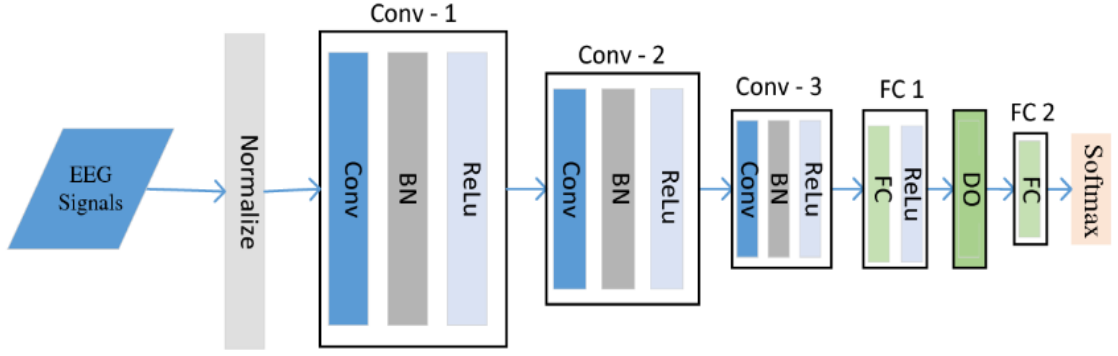
Figure 2. ID-CNN framework for classification

Let the input signal's sequence be s'i in which $i = 1,2,3,....ni$ and filter be f_i in which $i = 1,2,3,....m$. Herein, the signal sequence's length ni remains greater than the filter's length m. The filter will be executed centered upon the former layer's input features via a limited convolution mechanism. The 1D-CNN's convoluted output x_i is expressed as,

$$x_i = \sum_{g=1}^{m} f_g \times s_{i-g+1} \qquad (7)$$

In above equation (7), each neuron in the dth layer is evaluated with the local window $(d-1)^{th}$ layer for the local connected network. The estimation in the network is based on non-linear activation function $af(s)$ in the convolutional layer. With the 1D-CNN paradigm the activation function is employed with the higher module convergerce denoted as in equation (8)

$$af(s') = \max(0, s') \qquad (8)$$

Additionally, the qth neuron's input of the dth layer is formulated as,

$$c_q^d = af(\sum_{r=1}^{m} f_r^d \times c_{q-r+m}^{d-1} + h_d)$$

$$= af(f^d \times c_{(q-m+1):q}^{d-1} + h_d) \qquad (9)$$

In the aforesaid formula, the offset criteria are regarded to be h^q in which $q = 1,2,3,....ni$, and the mth dimension filter is called $f^d \in R^m$ that remains similar for entire neurons inside the convolution layer. 1D-CNNs effectively perform in 1D EEG signals because of the disparate benefits such as low arithmetical intricacy having easy set procedures and effortless training and application alongside some hidden layers.

The 1D convolution layer's outputs out of the initial CNN layer or block are regarded to be an input in the secondary CNN layer or block. In this secondary layer, BM is implemented upon the output out of the former CNN layer, and the former Conv1D configuration is enforced into this layer. An additional sub-block called max pooling layer (MaxPooling1D) is included finally in the secondary CNN layer wherein MaxPooling1D is configured alongside a sliding window having height three. As a result, in the tertiary CNN layer, a few modifications are done in the Conv1D layers wherein the Conv1D is configured alongside 160 sliding windows (feature detector) having five as kernel dimension, or height and a mean pooling layer having similar sliding window height that is employed rather than max pooling layer. In the following phase, a dropout layer is regarded as having a rate of 0.5 for preventing overfitting. Lastly, a completely linked layer called dense layer having a softmax activation is employed for producing probabilistic dispensation through the 2 classes for obtaining classification outcomes.

3.4.1 Convolutional layer (Maxpool1D):

In the convolutional output the feature mapping is performed in the Conv 1D layers those act as the input for the 1D max pooling layer, which minimizes the feature map for maintaining the maximal value of the feature map in the window patch in pool dimensions. The features are either shifted based on the convolutional layer as illustrated in figure 3. The maximal pooling is represented as in equation (10)

$$c_h^l = max c_p^{l-1} . r_h \qquad (10)$$

in which r_h represents the pooling area having index h. In our study, the pool dimension and stride's value are considered as two. A representation of the max pooling mechanism having these criteria is provided in which $c_{m1} = \max(c_1, c_2); \quad c_{m2} = \max(c_3, c_4); c_{m3} = \max(c_5, c_6)$.
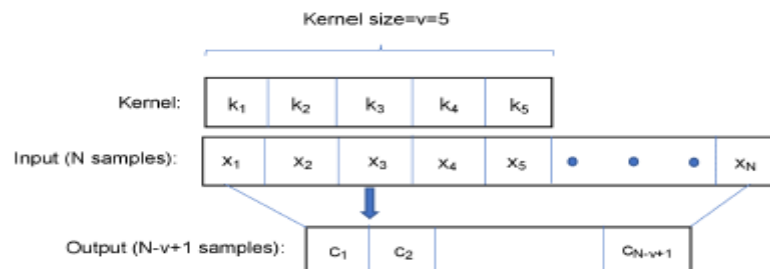

Figure 3. Representation of convolution mechanism

3.4.2 Dropout and flatten layer

The flatten layer converts the input data as a unidimensional vector that would be supplied to the completely linked/dense layer. A dropout criterion is included subsequent to the flatten layer that assists the framework for universalizing splendidly by lessening overfitting while doing the training procedure. It is attained by haphazardly fixing the activations of a few nodes to 0 as defined by a dropout rate. Our study employs a 0.25 dropout rate.

3.4.3 Classification with Dense layer

The flattened output is provided as an input to the subsequent layer, that is, dense/completely joined layer that generates the classification output having the size $M \times 1$ in which M portrays the classes' quantity. Substantially, the layer mechanism could be portrayed by,

$$output = \sigma(< input, w_d > + b_d) \qquad (11)$$

in which $(< input, w_d >$ portrays the dot product betwixt weight vector w_d employed in the layer and input, b_d portrays the bias vector for the layer, and σ portrays the activation function. This study employs the two, activation function as sigmoid and softmax to perform the classification in terms of binary and multi-class. The activation function in the sigmoid is represented as in equation (12)

$$\sigma(z) = \frac{1}{1+e^{-z}} \qquad (12)$$

The sigmoidal function generates the output in binary form based on the computed probability value for the classification in binary form according to the class label either zero or one. The activation function in the softmax layer is represented in equation (13)

$$Softmax(z)_i = p_i = \frac{\exp(z)_i}{\sum_{j=1}^{m} \exp(z)_j} \qquad (13)$$

in which zi portrays the output vector's i^{th} component of the former layer z. To determine the value of pi between zero and one, the numerator is normalised by the sum of all exponential expressions from 1 to M. For multiple class categorization, this layer creates categorical class labels. For this layer, we don't use bias vectors, and the weights are initialised using the glorot uniform initialise.

Still, for smaller periods of processing length, the proffered framework attains resembling precisions for disparate mental tasks classifications. It remains beneficial for the schemes in which swift reply is required, for instance, BCI and neurofeedback schemes. Additionally, this could be noticed that the classification precision remains greater for 2 conv1D layers when correlated with single or many 2 layers in the proffered framework. Hence, 2 conv1D layers remain ideal in the proffered framework for the mental tasks classification.

4.Performance analysis

The results of the experiment are analysed using Python software, using the following parameters: accuracy, precision, recall, f1-score, and False Positive Rate (FPR). These parameters are compared with existing methods such as Decision Tree Algorithm (DTA)(existing-1)[28], Hybrid Classification Model (HCM))(existing-2)[29],Morelette wavelets Method (MWM))(objective-1)[30], and Convolution Neural Network (CNN))(objective-2), with proposed 1D-CNN.The formulas for the chosen parameters are given below:

A comparison of the accuracy of different existing DTA, HCM,MWM,CNN methods and proposed ID-CNN method is shown in table1

Table 1. Comparison of the accuracy

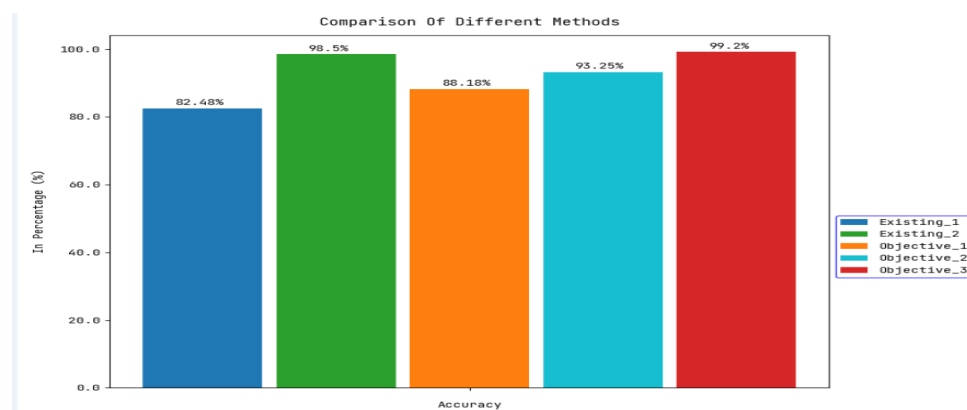| Count of epochs	DTA	HCM	MWM	CNN	1D-CNN
100	0.82	0.95	0.85	0.92	0.98
200	0.81	0.98	0.86	0.93	0.97
300	0.83	0.96	0.85	0.94	0.99
400	0.82	0.96	0.88	0.93	0.96
500	0.81	0.95	0.87	0.92	0.97

Figure.4 Correlation of accuracy

The figure 4 illustrates the comparison of accuracy between DTA, HCM,MWM,CNN methods and proposed ID-CNN method. Analytical procedures are shown on the X axis, while the percentage of correctness is plotted on the Y axis. When compared, existing DTA, HCM,MWM,CNN methods achieve 0.8248, 0.98, 0.8818 and 0.9325while the proposed ID-CNN method achieves 0.992 of accuracy.

A comparison of the precision of different existing DTA, HCM,MWM,CNN methods and proposed ID-CNN method is shown in table 2.

Table 2. Comparison of the of precision

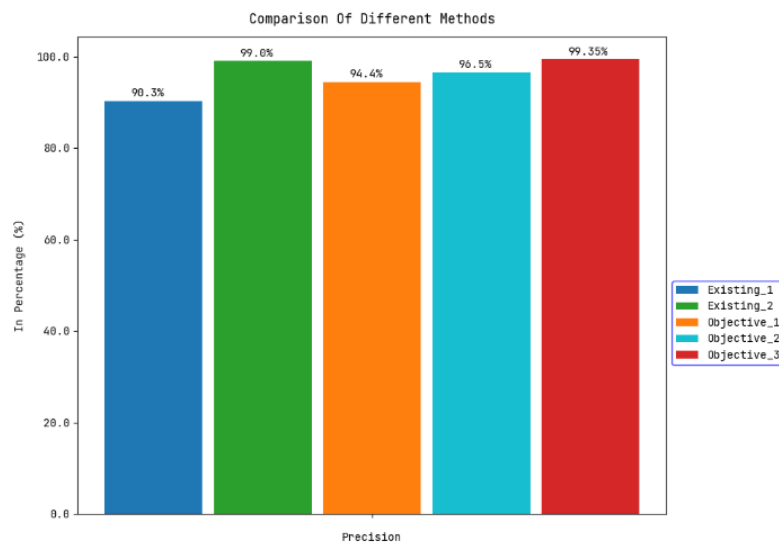| Count of epochs	DTA	HCM	MWM	CNN	1D-CNN
100	0.98	0.98	0.95	0.95	0.98
200	0.97	0.99	0.94	0.96	0.96
300	0.96	0.98	0.95	0.95	0.99
400	0.97	0.97	0.94	0.94	0.97
500	0.96	0.99	0.93	0.94	0.97

Figure.5 Correlation of precision

The figure 5 illustrates the comparison of precision between DTA, HCM,MWM,CNN methods and proposed ID-CNN method . The X axis depicts the different ways of analysis, while the Y axis displays the degree of precision attained. When compared, existing DTA, HCM,MWM,CNN methods achieve 0.908, 0.99, 0.944 and 0.965while the proposed ID-CNN method achieves 0.993of precision.

A comparison of the recall of different existing DTA, HCM,MWM,CNN methods and proposed ID-CNN method is shown in table 3.

Table 3. Comparison of the recall

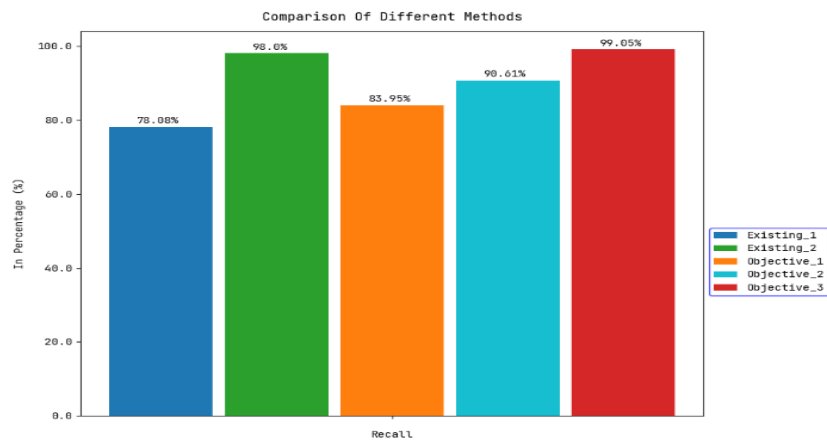| Count of epochs	DTA	HCM	MWM	CNN	1D-CNN
100	0.78	0.96	0.83	0.97	0.99
200	0.77	0.97	0.82	0.96	0.98
300	0.79	0.98	0.83	0.98	0.98
400	0.76	0.96	0.84	0.94	0.99
500	0.79	0.98	0.84	0.97	0.97

Figure.6 Correlation of recall

The figure 6 illustrates the comparison of recall between DTA, HCM,MWM,CNN methods and proposed ID-CNN method. Analytical methodologies are shown on the X axis, while the recall % is shown on the Y axis. When compared, existing DTA, HCM,MWM,CNN methods achieve 0.7808, 0.98, 0.8395and 0.9061 while the proposed ID-CNN method achieves 0.9905 of recall.

A comparison of the F-measure of different existing DTA, HCM,MWM,CNN methods and proposed ID-CNN method is shown in table 4.

Table 4. Comparison of the F-measure

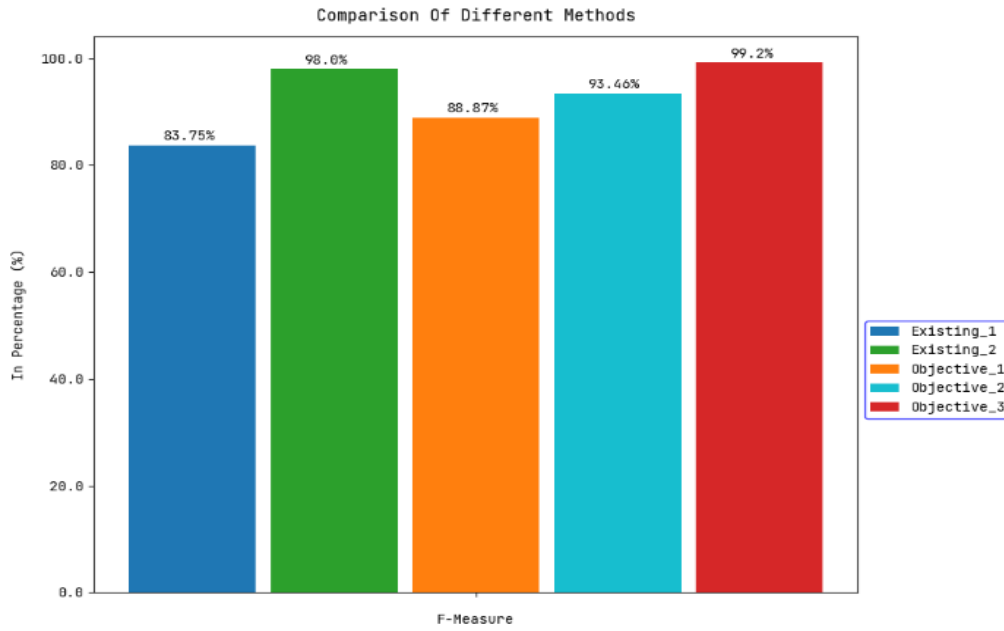| Count of epochs	DTA	HCM	MWM	CNN	1D-CNN
100	0.84	0.98	0.89	0.94	0.98
200	0.83	0.87	0.88	0.93	0.99
300	0.94	0.96	0.87	0.94	0.98
400	0.82	0.97	0.88	0.94	0.97
500	0.84	0.98	0.87	0.93	0.98

Figure.7 Correlation of F-measure

The figure 7 illustrates the comparison of F-measure between DTA, HCM,MWM,CNN methods and proposed ID-CNN method. The Y axis displays the F-measure as a percentage, while the X axis displays the different techniques of analysis. When compared, existing DTA, HCM,MWM,CNN methods achieve 0.8375, 0.98, 0.8887and 0.9346while the proposed ID-CNN method achieves 0.992of F-measure

A comparison of the False Positive Rate (FPR) of different existing DTA, HCM,MWM,CNN methods and proposed ID-CNN method is shown in table 5.

Table.5.Comparison of the False Positive Rate (FPR)

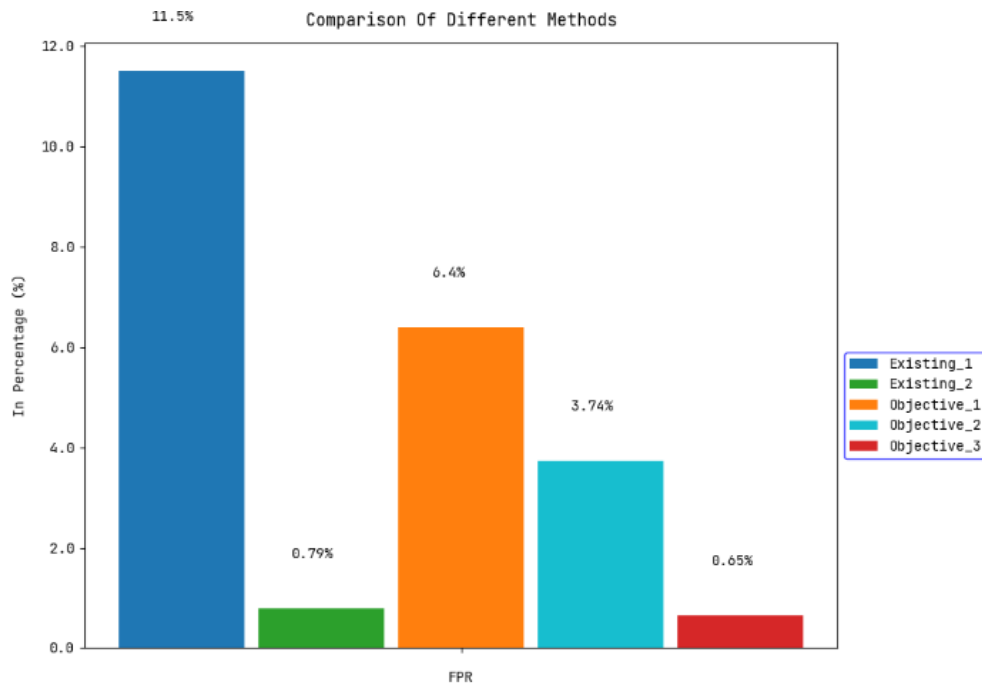| Count of epochs	DTA	HCM	MWM	CNN	1D-CNN
100	0.12	0.03	0.04	0.03	0.003
200	0.11	0.02	0.05	0.02	0.004
300	0.13	0.01	0.06	0.01	0.006
400	0.11	0.002	0.04	0.03	0.003
500	0.10	0.007	0.03	0.02	0.004

Figure.8 Correlation of FPR

The figure 8 illustrates the comparison of FPR between DTA, HCM,MWM,CNN methods and proposed ID-CNN method The Y axis displays the FPR as a percentage, while the X axis depicts the different techniques of analysis. When compared, existing DTA, HCM,MWM,CNN methods achieve 0.115, 0.0079, 0.064 and 0.0374 while the proposed ID-CNN method achieves 0.0065 of FPR
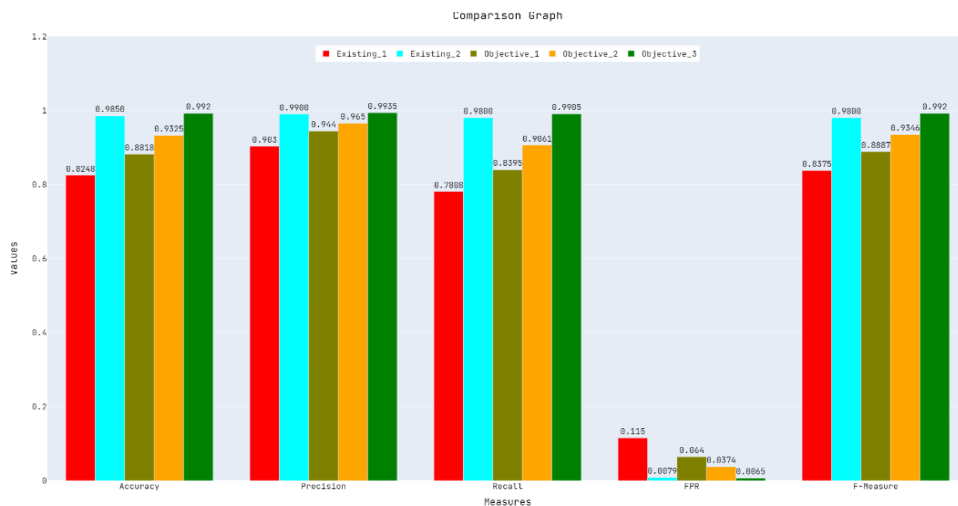

Figure.8 Comprehensive correlation betwixt prevailing and proffered methodologies

The figure 9 illustrates the Comprehensive correlation betwixt prevailing and proffered methodologies where X axis shows various parameters used for analysis and Y axis shows

the values obtained in percentage. When compared, existing DTA, HCM,MWM,CNN methods the proposed ID-CNN method achieves better results.

A comparison of the Comprehensive comparative analysis of different existing DTA, HCM,MWM,CNN methods and proposed ID-CNN method.

Table 6. Comparison of the Comprehensive comparative analysis

Measures	DTA (Existing_1)	HCM (Existing_2)	MWN (objective_1)	CNN (objective_2)	Proposed (objective_3)
Accuracy	0.8248	0.98	0.8818	0.9325	0.992
Precision	0.908	0.99	0.944	0.965	0.993
Recall	0.7808	0.98	0.8395	0.9061	0.9905
FPR	0.115	0.0079	0.064	0.0374	0.0065
F-measure	0.8375	0.98	0.8887	0.9346	0.992

5.Conclusion

In this paper we propose a one-dimensional convolutional neural network (1D-CNN) architecture for mental task identification and classification, The suggested architecture comprises of a few layer network with feature extraction and artefact suppression. As shown by varied activation weights, our proposed CNN architecture has developed discriminating feature maps for baseline and distinct mental task categorization, resulting in good accuracy. The suggested 1D-CNN achieves accuracy of 0.992, precision of 0.993, recall of 0.9905, FPR of 0.0065, and F-measure of 0.992. In the future, we want to investigate the performance of the suggested architecture in the absence of EEG data, as well as to build it on real-time processor integrates with the real-time latency estimation and categorization of the poer consyumption for the estimation of mental tasks.

REFERENCE

1. L. Shoker, S. Sanei, J. Chambers, Artifact removal from electroencephalograms using a hybrid BSS-SVM algorithm, IEEE Signal Processing Letters 12 (10) (2005) 721–724.
2. H. Nolan, R. Whelan, R.B. Reilly, FASTER: Fully Automated Statistical Thresholding for EEG artifact Rejection, Journal of Neuroscience Methods 192 (1) (2010) 152–162.
3. R. Mahajan, B.I. Morshed, Unsupervised Eye Blink Artifact Denoising of EEG Data with Modified Multiscale Sample Entropy, Kurtosis, and Wavelet-ICA, IEEE Journal of Biomedical and Health Informatics 19 (1) (2015) 158–165.
4. U. Srilakshmi, J Manikandan, Thanmayee Velagapudi, Gandla Abhinav, Tharun Kumar, & Dogiparthy Saideep. (2024). A New Approach to Computationally- Successful Linear and Polynomial Regression Analytics of Large Data in Medicine. Journal of Computer Allied Intelligence, 2(2), 35-48.

5. Matta V., Di Mauro M., Longo M., (2016), Botnet Identification in Randomized DDoS Attacks. In Proc. of IEEE EUSIPCO16, pp. 2260-2264 Budapest (Hungary), Aug./Sept. 2016.

6. Md. Mamun, Mahmoud Al-Kadi, Mohd. Marufuzzaman, Effectiveness of Wavelet Denoising on Electroencephalogram Signals, Journal of Applied Research and Technology 11 (1) (2013) 156–160

7. Srinivasa Sai Abhijit Challapalli, Bala kandukuri, Hari Bandireddi, & Jahnavi Pudi. (2024). Profile Face Recognition and Classification Using Multi-Task Cascaded Convolutional Networks. Journal of Computer Allied Intelligence, 2(6), 65-78.

8. Graves A, Mohamed A and Hinton G 2013 Speech recognition with deep recurrent neural networks 2013 IEEE Int. Conf. on Acoustics, Speech and Signal Processing pp 6645–9

9. Greenspan H, van Ginneken B and Summers R M 2016 Guest editorial deep learning in medical imaging: overview and future promise of an exciting new technique IEEE Trans. Med. Imaging 35 1153–9

10. Baltatzis V, Bintsi K-M, Apostolidis G K and Hadjileontiadis L J 2017 Bullying incidences identification within an immersive environment using HD EEG-based analysis: a swarm decomposition and deep learning approach Sci. Rep. 7 17292

11. Swapna Saturi, & Sandhya Banda. (2024). Advanced Lung Disease Detection and Classification Using Ge-U-Net-ODLwith Gabor Filters and Entropy-Based Feature Selection. Journal of Sensors, IoT & Health Sciences, 2(2), 69-86.

12. Van Leeuwen K G, Sun H, Tabaeizadeh M, Struck A F, Van Putten M J A M and Westover M B 2019 Detecting abnormal electroencephalograms using deep convolutional networks Clin. Neurophysiol. 130 77–84

13. U. Satija, B. Ramkumar, M. S. Manikandan, "Automated ECG noise detection and classification system for unsupervised healthcare monitoring," IEEE Journal of Biomedical and Health Informatics, vol. 22, no. 3, pp. 722 - 732, May 2017. I.F.-3.45.

14. Srinivasa Sai Abhijit Challapalli. (2024). Sentiment Analysis of the Twitter Dataset for the Prediction of Sentiments. Journal of Sensors, IoT & Health Sciences, 2(4), 1-15.

15. P. Croce et.al., "Deep convolutional neural networks for feature-less automatic classification of independent components in multi-channel electrophysiological brain recordings," in IEEE Transactions on Biomedical Engineering, vol. 66, no. 8, pp. 2372-2380, Aug. 2019.

16. D. Peng et. al., "A novel deeper one-dimensional CNN with residual learning for fault diagnosis of wheel set bearings in high-speed trains," in IEEE Access, vol. 7, pp. 10278-10293, 2019.

17. M. P´erez-Enciso et. al., "A guide on deep learning for complex trait genomic prediction," Genes, vol. 10, no. 7, p. 553, 2019

18. Liang J, Lu R, Zhang C, Wang F (2016): Predicting Seizures fromElectroencephalography Recordings: A Knowledge TransferStrategy. In 2016 IEEE International Conference on HealthcareInformatics (ICHI), pp 184–191.

19. Judith, A. M., Priya, S. B., & Mahendran, R. K. (2022). Artifact Removal from EEG signals using Regenerative Multi-Dimensional Singular Value Decomposition and Independent Component Analysis. Biomedical Signal Processing and Control, 74, 103452.

20. Islam, M. K., Ghorbanzadeh, P., & Rastegarnia, A. (2021). Probability mapping based artifact detection and removal from single-channel EEG signals for brain–computer interface applications. Journal of Neuroscience Methods, 360, 109249.

21. Jamil, Z., Jamil, A., & Majid, M. (2021). Artifact removal from EEG signals recorded in non-restricted environment. Biocybernetics and Biomedical Engineering, 41(2), 503-515.

22. Mathe, M., Padmaja, M., & Krishna, B. T. (2021). Intelligent approach for artifacts removal from EEG signal using heuristic-based convolutional neural network. *Biomedical Signal Processing and Control*, *70*, 102935.

23. Lin, G., Zhang, J., Liu, Y., Gao, T., Kong, W., Lei, X., & Qiu, T. (2022). Ballistocardiogram artifact removal in simultaneous EEG-fMRI using generative adversarial network. *Journal of Neuroscience Methods*, *371*, 109498.

24. Webb, L., Kauppila, M., Roberts, J. A., Vanhatalo, S., & Stevenson, N. J. (2021). Automated detection of artefacts in neonatal EEG with residual neural networks. *Computer Methods and Programs in Biomedicine*, *208*, 106194.

25. Sheoran, P., & Saini, J. S. (2020). A new method for automatic electrooculogram and eye blink artifacts correction of EEG signals using CCA and NAPCT. *Procedia Computer Science*, *167*, 1761-1770.

26. Sun, W., Su, Y., Wu, X., & Wu, X. (2020). A novel end-to-end 1D-ResCNN model to remove artifact from EEG signals. *Neurocomputing*, *404*, 108-121.

27. Dora, C., & Biswal, P. K. (2020). Correlation-based ECG artifact correction from single channel EEG using modified variational mode decomposition. *Computer Methods and Programs in Biomedicine*, *183*, 105092.

28. Shan Guan, Kai Zhao, Shuning Yang, "Motor Imagery EEG Classification Based on Decision Tree Framework and Riemannian Geometry", *Computational Intelligence and Neuroscience*, vol. 2019, Article ID 5627156, 13 pages, 2019.

29. Ketu S, Mishra PK. Hybrid classification model for eye state detection using electroencephalogram signals. Cogn Neurodyn. 2022 Feb;16(1):73-90.

30. Padmini Chattu and Dr. C.V.P.R. Prasad ,"Removing Artifacts in EEG Data Based On Wavelets And Neural Networks," Journal of Theoretical and Applied Information Technology ,vol.99,no 22,pp.5470-5478,2021.